Molecular Therapy
Nucleic Acids
Original Article

Use of Heterologous Vesiculovirus G Proteins Circumvents the Humoral Anti-envelope Immunity in Lentivector-Based *In Vivo* Gene Delivery

Altar M. Munis,[1,2,5] Giada Mattiuzzo,[3] Emma M. Bentley,[3] Mary K. Collins,[1,4] James E. Eyles,[1] and Yasuhiro Takeuchi[1,2]

[1]Division of Advanced Therapies, National Institute for Biological Standards and Control, South Mimms EN6 3QG, UK; [2]Division of Infection and Immunity, University College London, London WC1E 6BT, UK; [3]Division of Virology, National Institute for Biological Standards and Control, South Mimms EN6 3QG, UK; [4]Okinawa Institute of Science and Technology, Okinawa 904-0412, Japan

Vesicular stomatitis virus Indiana strain glycoprotein (VSVind.G) mediates broad tissue tropism and efficient cellular uptake. Lentiviral vectors (LVs) are particularly promising, as they can efficiently transduce non-dividing cells and facilitate stable genomic transgene integration; therefore, LVs have an enormous untapped potential for gene therapy applications, but the development of humoral and cell-mediated anti-vector responses may restrict their efficacy. We hypothesized that G proteins from different members of the vesiculovirus genus might allow the generation of a panel of serotypically distinct LV pseudotypes with potential for repeated *in vivo* administration. We found that mice hyperimmunized with VSVind.G were not transduced to any significant degree following intravenous injection of LVs with VSVind.G envelopes, consistent with the thesis that multiple LV administrations would likely be blunted by an adaptive immune response. Excitingly, bioluminescence imaging studies demonstrated that the VSVind-neutralizing response could be evaded by LV pseudotyped with Piry and, to a lesser extent, Cocal virus glycoproteins. Heterologous dosing regimens using viral vectors and oncolytic viruses with Piry and Cocal envelopes could represent a novel strategy to achieve repeated vector-based interventions, unfettered by pre-existing anti-envelope antibodies.

INTRODUCTION

Lentiviral vectors are promising gene delivery systems in the treatment of both hereditary and acquired diseases.[1] However, *in vivo* lentiviral vector (LV) gene therapy is still at a preclinical development stage,[2–5] while *ex vivo* therapies using hematopoietic stem and progenitor cells and T cells are in clinical use.[6–10] One of the major hurdles in *in vivo* LV gene therapy advancement is the immune responses directed toward LVs, which limit the efficacy and safety of the therapy.[1,11] Likewise, the primary immune response elicited following the administration of vesicular stomatitis virus Indiana strain (VSVind) has led to the generation of strongly neutralizing antibodies, and it has limited the efficacy of the oncolytic therapy, precluding repeated administrations.[12,13]

It has been reported that systemic administration of LVs induces a primary immune response through CD4+ T cell-mediated mechanisms directed toward the LV envelope and/or core proteins.[14,15] In this case, although the efficacy and safety of the initial vector administration should not be affected, the effect of subsequent doses of therapy may be limited. Although the development of these antibodies did not limit transduction efficiency, strongly neutralizing antibodies toward the matrix (p17) and capsid proteins (p24) limited the efficacy of a subsequent administration of the same vector.[14] On the other hand, the effects of neutralizing anti-envelope antibodies to LV efficacy remain to be fully explored in animal models.[16]

LV-derived antigens, such as envelope and capsid proteins, are expected to induce robust immune responses, both in humans and animal models, following intravenous administration.[14] While the acute effector phase will eventually subside, immunological memory is likely to be protracted due to development of central memory T cells, memory B cells, and long-lived plasma cells, thereby rendering subsequent doses of the same vector less effective.[17,18] As LVs may also activate innate immune responses in parallel to adaptive immune pathways, their administration may exacerbate any anti-vector immune responses, due to the induction of inflammatory pathways.[19]

Here we have examined the inhibitory effects of pre-existing anti-envelope immunity on subsequent LV administrations pseudotyped with the gold standard vesicular stomatitis virus Indiana strain glycoprotein (VSVind.G), and we demonstrated that diverse vesiculovirus G proteins (VesGs), namely that of Cocal virus (COCV), Maraba virus (MARAV), and Piry virus (PIRYV), may allow LVs to circumvent this pre-existing humoral immunity.

Received 11 March 2019; accepted 15 May 2019;
https://doi.org/10.1016/j.omtn.2019.05.010.

[5]Present address: Gene Medicine Group, John Radcliffe Hospital, University of Oxford, Oxford OX3 9DU, UK

Correspondence: Altar M. Munis, Division of Advanced Therapies, National Institute for Biological Standards and Control, South Mimms EN6 3QG, UK.
E-mail: altar.munis@ndcls.ox.ac.uk

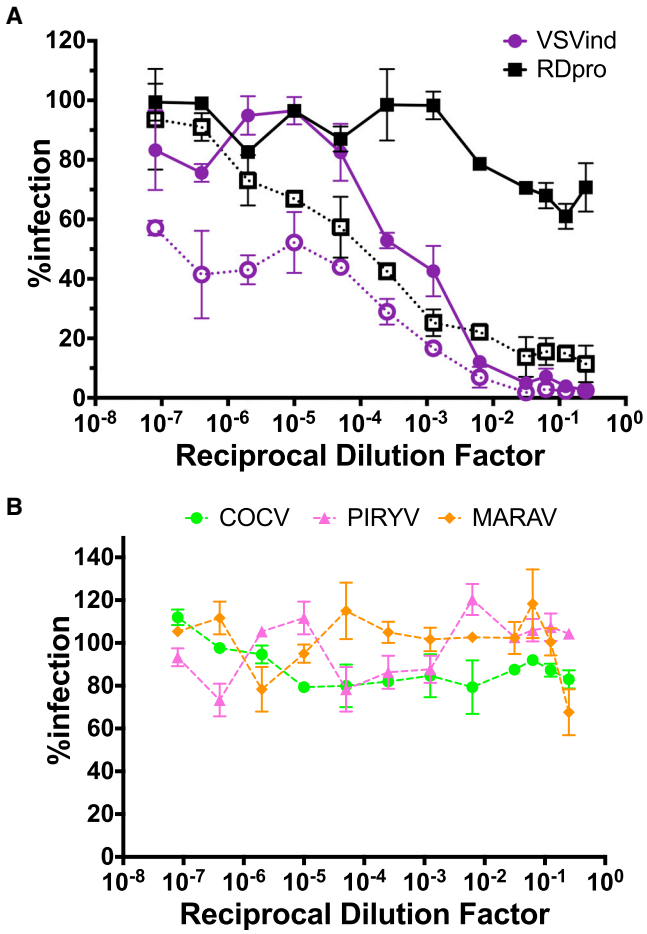

Figure 1. Intravenous LV Injection Prompts a Specific Neutralizing Anti-envelope Response

(A) Neutralization activity of pooled sera on VSVind.G- and RDpro-pseudotyped LVs pre- (dotted lines with clear symbols) and post-adsorption (solid lines with filled symbols) with HEK293T cells. (B) Neutralization activity of pooled sera on VesG-LV post-adsorption. Data shown represent the mean ± SD of three repeats performed in duplicates.

RESULTS

Intravenous LV Administration Induces Envelope-Specific Neutralizing Antibodies

To determine whether intravenous (i.v.) LV administration would lead to the production of envelope-specific neutralizing antibodies, three female BALB/c mice were injected with 5×10^7 transducing units (TU)/mouse VSVind.G-pseudotyped LVs (VSVind.G-LV), and blood samples were collected after 21 days. Sera were isolated and pooled, and neutralizing activity was determined through an *in vitro* LV neutralization assay previously described (Figure 1).[20] VSVind.G-LV infection was blocked in a dose-dependent manner; however, a similar effect was also observed for LVs pseudotyped with the unrelated feline endogenous retrovirus RD114-derived (RDpro) envelope (Figure 1A, dotted lines). This unspecific neutralizing activity suggested that the inhibition of LV infection might be due to antibodies directed against proteins on the vector surface acquired from the producer cells during the LV production, namely, host-cell proteins. This anti-HEK293T response could be against proteins encoded by the human leukocyte antigen (HLA) complex, as a similar major histocompatibility complex class I (MHC-I)-directed immune response has been reported in hemophilia B mouse models.[21]

To isolate the anti-VSVind.G response, 150 µL pooled sera was first incubated with 1×10^7 HEK293T cells on ice for 1 h, and then it was submitted to neutralization assay analysis. This incubation successfully removed anti-HEK293T antibodies, as, after adsorption, the neutralizing activity against RDpro-LV was lost. This then revealed a strongly neutralizing anti-VSVind.G response (Figure 1A, solid lines), which was specific to VSVind.G, as LVs pseudotyped with the other three VesGs remained infectious (Figure 1B).

Pre-existing Anti-envelope Immunity Blocks the Subsequent LV Administration

A challenge study was then designed to explore the mechanism behind the observed neutralizing humoral response. However, because *in vivo* administration of these LV constructs would elicit an anti-HEK293T response, thereby confounding interpretation of infectivity data following any subsequent LV exposure, a different strategy was used to induce pre-existing immunity: repeated injection of adjuvanted G protein (Gth) isolated from wild-type VSVind.[22,23] More specifically, BALB/c mice were bi-laterally immunized subcutaneously (s.c.) with 4 µg Gth protein mixed with Sigma Adjuvant System Oil (for a total of 8 µg protein/mouse). Mice were boosted 2 weeks following the primary immunization, using the same procedure (Figure 2A). Then 3 weeks later, one of the immune response groups (immunization + challenge [IC]) was challenged by i.v. injection of 5×10^7 TU/mouse VSVind.G-LV, encoding both firefly luciferase (FLuc) and EGFP (Figure 2D). Immunization-only (IO) and challenge-only (CO) groups were either only immunized and received PBS injections or received a vector dose following immunization and boost with the adjuvant only. The study was terminated 21 days post-challenge, at which time terminal bleeds were collected. During the study, none of the mice showed signs of distress (observation), and no substantial changes in body weights were measured.

Prior to the LV challenge, the serum antibody levels in immunized mice were assessed (data not shown), and the induced immune response was characterized to ensure a VSVind.G-specific neutralizing response was elicited. Characterizations of pre-challenge serum samples revealed that the induced humoral response was neutralizing and VSVind.G specific (Figures 2B and 2C). Analyses revealed that the antibody response induced via Gth immunization exhibited similar properties to the one elicited by i.v. administration of LV. Following VSVind.G-LV challenge, luciferase expression was monitored via bioluminescence imaging for 21 days (Figures 2E and 2F). At day 2 post-challenge, a strong luciferase signal could be detected in CO mice, mainly localized at the liver, spleen, and inguinal and

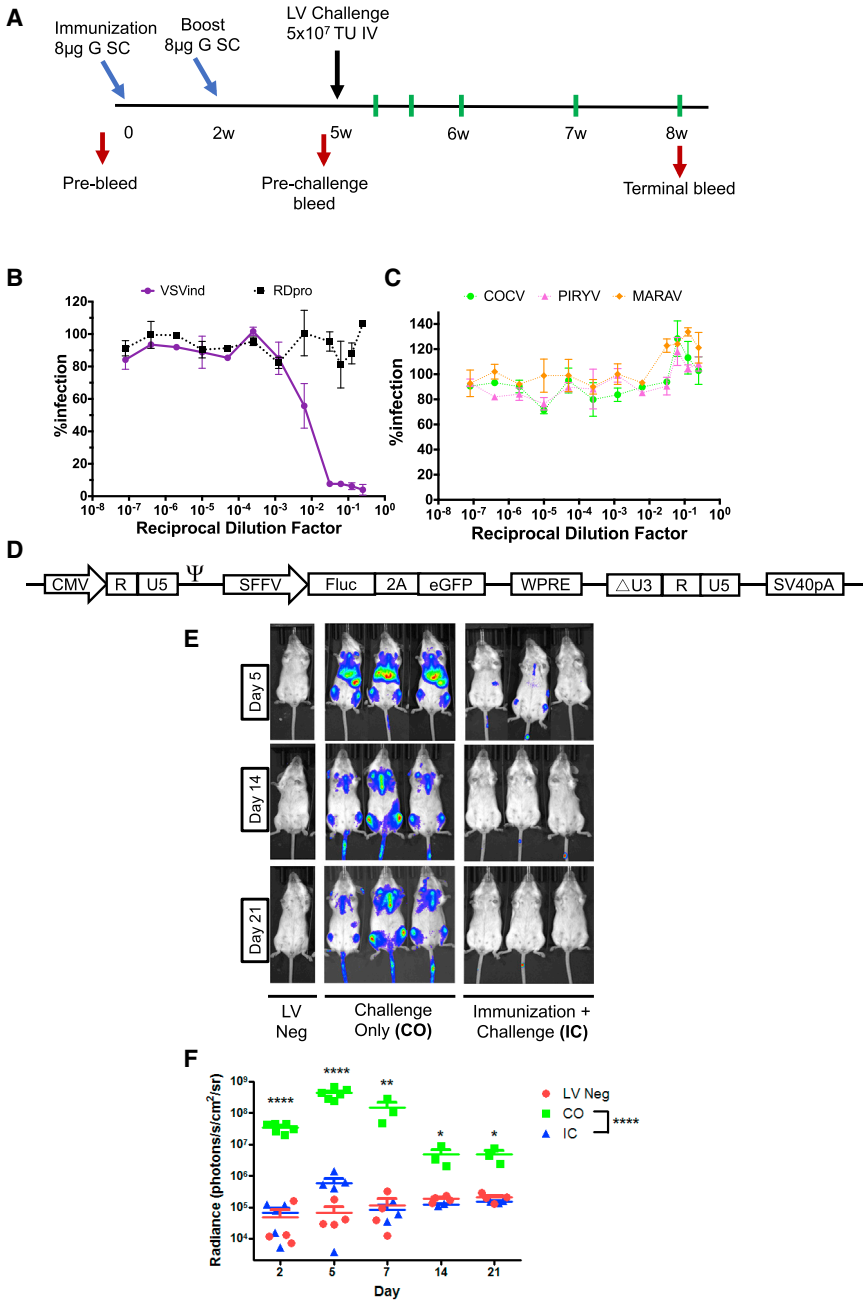

Figure 2. Pre-existing Anti-VSVind.G Immunity Hinders the Efficacy of a Subsequent VSVind.G-LV Injection

(A) Timeline of the study. Immunization and boost points are identified by light blue arrows, while the black arrow indicates the time of LV challenge. Red arrows designate the times at which blood samples were collected through tail vein bleeds. Green lines show the days on which mice were imaged. At termination of the study, terminal bleeds and post-mortem organ harvest were performed. w, weeks. Neutralization activity of pooled IO sera on (B) VSVind.G- and RDpro-pseudotyped LVs and (C) other VesG-LVs. Data shown represent the mean ± SD of three repeats performed in duplicates. (D) Schematic representation of the LV vector construct. (E) Representative bioluminescence images of transduced and naive mice at the three time points of days 5, 14, and 21 post-challenge. Localization and the intensity of the luciferase signal are depicted in a heatmap. (F) Photon emission from each mouse was quantified as radiance (p/s/cm^2/sr) post-imaging, using region of interest analysis in Living Image software. Each dot represents a mouse and the horizontal bar shows the median. Two-way ANOVA followed by Bonferroni multiple comparison test was performed to analyze the significance of luciferase expression differences in LV-negative, CO, and IC mice at each imaging time point (indicated on the graph) as well as overall throughout the study (indicated in the legend). In all comparisons, the differences between LV-negative and IC samples were not significant (data not shown). (****$p < 0.0001$, **$p < 0.01$, *$p < 0.05$). Neg, negative.

auxiliary lymph nodes (Figure 2E). This signal was sustained for 2 weeks. On day 14, clearance of the luciferase signal from the liver and spleen was observed, however, luciferase expression in the lymph nodes and the tracheal region remained constant until the termination of the study. This was confirmed via post-mortem analysis of the luciferase activity in the organs (data not shown). A similar vector clearance has been previously reported in the liver.[24]

In the CO group, overall measured radiance levels throughout the study were significantly higher compared to that of the IC group ($p < 0.0001$) (Figure 2F). In addition, a multiple comparison of each imaging time point revealed significant differences in luciferase expression in the CO group compared to the IC group and naive mice (LV negative) (Figure 2F). In the IC group, luciferase expression could not be detected, and the radiance of mice in the IC group remained comparable to that of LV-negative mice for the whole study (overall average radiances 2.01×10^5 and 1.24×10^5 p/s/cm^2/steradian [sr], respectively). Thus, the induced anti-envelope immunity significantly reduced the efficacy of a subsequent viral vector injection utilizing the envelope homologous to the immunogen.

LV Challenge Acts as a Boost for Pre-existing Anti-envelope Immunity

The LV challenge of pre-immunized mice may boost the immune system, prompting an even stronger response that blocks vector transduction. To investigate this, we explored the neutralizing activity of the sera isolated from IC mice sacrificed on day 21 post-challenge (IC-D21 mice). As previously described, sera were pooled, adsorbed

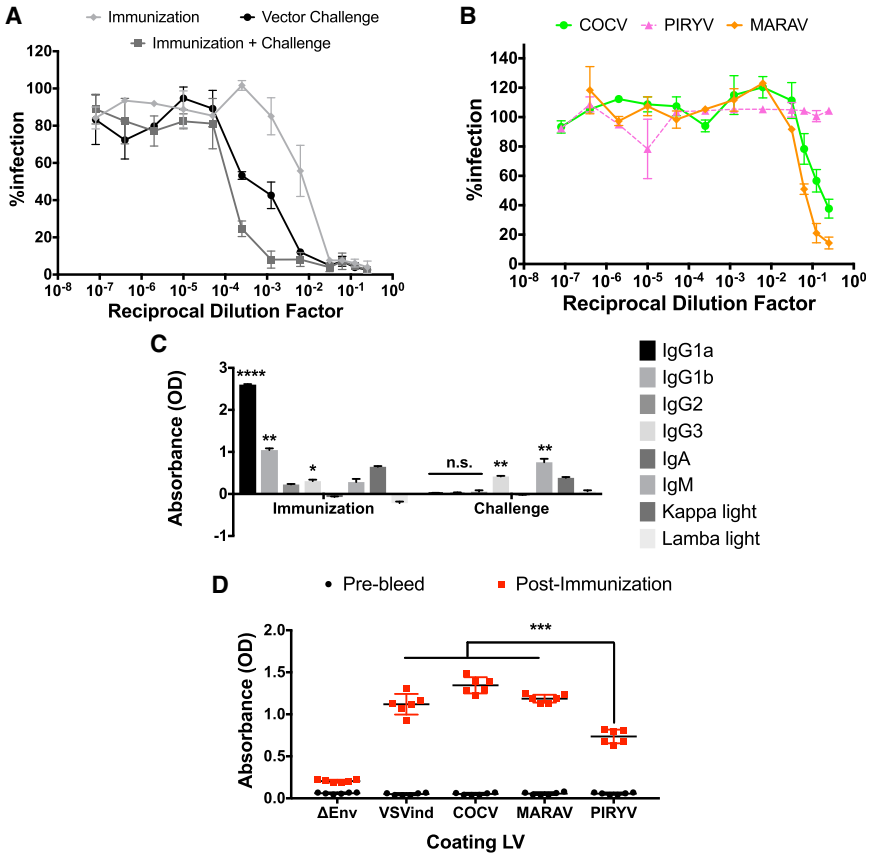

Figure 3. LV Challenge of Pre-immunized Mice Strengthens the Neutralizing Activity

(A) The strength of VSVind.G-LV neutralization activity elicited by Gth immunization, LV challenge, and the combination of both. The calculated IC_{50} values were as follows: immunization (IO sera pooled), 6.96×10^{-3}; vector challenge (CO sera pooled), 1.20×10^{-3}; and immunization + challenge (IC sera pooled), 1.51×10^{-4}. (B) Cross-neutralizing activity of sera isolated from IC terminal bleeds. Solid lines signify the neutralization effect observed, while the dotted lines indicate the lack of neutralization. Data shown represent the mean ± SD of three repeats performed in duplicates. To calculate IC_{50} values, curves were fitted using the software GraphPad Prism 5 modeled as an [inhibitor] versus response curve with variable hill slopes. (C) Isotypes of antibodies produced following Gth immunization versus VSVind.G-LV challenge. Wells were coated overnight with 50 ng/well recombinant VSVind.G, and they were incubated with pooled serum samples isolated from pre- and terminal bleeds. The absorbances measured from pre-bleed serum samples were regarded as background and subtracted from terminal bleed sera. One-way ANOVA with Tukey's multiple comparison post-test was performed to compare absorbance levels within the experimental groups (****$p < 0.0001$, **$p < 0.01$; n.s., not significant). Data shown represent mean ± SD of one experiment performed in triplicates. (D) Anti-VesG antibodies induced by Gth immunization-boost regimen. Sera obtained from pre-bleed and pre-challenge bleeds (i.e., post-immunization) were pooled, and the amounts of antibodies directed against the four VesGs were determined via LV-based ELISA. The amount of antibodies recognizing PIRYV.G was significantly less compared to the other three VesGs. One-way ANOVA followed by Holm-Sidak's multiple comparison post-test was performed to analyze the significance of the amount of anti-VesG antibodies produced via Gth immunization (***$p < 0.001$). Data shown represent mean ± SD from two experiments performed in duplicates.

to HEK293T cells, and incubated with VSVind.G- and VesG-pseudotyped LVs (Figure 3). As expected, i.v. LV injection to mice pre-immunized with Gth strengthened the neutralizing anti-envelope response, shifting the half maximal inhibitory concentration (IC_{50}) approximately 50-fold (from 0.007 to 0.0001) (Figure 3A). This response prompted by the combination of s.c. immunization and i.v. vector injection was ten times more potent than the one induced by LV challenge only (IC_{50} values of 0.0001 and 0.001, respectively).

To understand the difference in strength of antibody response to Gth immunization in comparison to VSVind.G-LV challenge, an immunoglobulin (Ig)-isotyping ELISA was performed on pooled serum samples (Figure 3C). This revealed that, while protein immunization induces a potent IgG1 response ($p < 0.0001$ for IgG1a and $p < 0.01$ for IgG1b), the increase in IgG levels following LV challenge was modest (not statistically significant). This indicates that the Gth immunization induced a stronger antigen-specific humoral response. On the other hand, following VSVind.G-LV administration there was a significant ($p < 0.01$) increase in IgG3 and IgM levels, indicative of activation of innate immunity and inflammatory pathways. Together, the data imply that, while LV challenge induced a modest anti-G accompanied with a strong anti-vector immune response, only a strong anti-protein antigen response was observed following Gth immunization.

Furthermore, to investigate the lack of cross-neutralization observed by sera acquired from immunized mice, we performed LV-based ELISAs (Figure 3D). Wells were coated with unenveloped (ΔEnv) and VesG-LVs and incubated with pooled serum samples. It revealed that the levels of antibodies present in the sera that recognized COCV.G and MARAV.G were similar to that of VSVind.G, which was significantly higher ($p < 0.001$) than that of PIRYV.G. This highlighted that, in a heterologous LV challenge, PIRYV.G-pseudoyped vectors might outperform both MARAV.G-LV and COCV.G-LV. In addition, the data demonstrated that, although no cross-neutralization was observed, cross-reactive antibodies were produced following Gth immunization.

Interestingly, although LV administration and Gth immunization alone did not produce any detectable cross-neutralizing antibodies against VesG (Figures 1B and 2C), sera of IC mice demonstrated weak neutralizing activity against MARAV.G- and COCV.G-pseudotyped LVs (IC_{50} 0.2 for COCV.G and 0.06 for MARAV.G)

(Figure 3B). This implied that MARAV.G and COCV.G, the closest phylogenetic relatives of VSVind.G,[25] may share several immunodominant epitopes, resulting in antibody cross-reactivity and neutralization.

Neutralizing Anti-envelope Response Can Be Circumvented Using Other VesGs

The VSVind.G-LV challenge study described above demonstrated that immunization with Gth elicited a sufficiently high-quality and high-magnitude immune response to prevent VSVind.G-LV-mediated transduction following vector administration i.v.. In fact, the IC_{50} of this neutralizing activity was approximately 10-fold higher (i.e., weaker neutralization) compared to that elicited by i.v. injection of VSVind.G-LV (Figure 3A). Likely this reflects the additional contribution of antibodies targeting non-G-related epitopes (e.g., anti-HEK293T, as described in the previous section). Nonetheless, these data imply sequential homologous LV-dosing regimens may well be heavily compromised by the development of anti-vector antibodies.

We proposed that a heterogeneous panel of envelopes could be utilized to sidestep this response, allowing for sequential injections to achieve desired levels of therapeutic transgene expression. To test this theory, four VesGs, VSVind.G, COCV.G, MARAV.G, and PIRYV.G, were selected. A study with the same Gth immunization-boost regimen was designed (Figure 4A). However, after priming the immune system for anti-VSVind.G immunity, mice were challenged with either VSVind.G-LV or other VesG-LVs. LV gene delivery efficacy was assessed utilizing bioluminescence imaging, and the study was terminated 7 days post-challenge.

Like the previous study, no adverse health effects were observed at any time point, and pre-challenge serum antibody levels were assessed via LV-based ELISA to ensure the presence of a VSVind.G-specific humoral response (data not shown).

Overall a similar biodistribution pattern was observed for all four pseudotypes (Figure 4B). In non-immunized mice, initial levels of reporter gene delivery by all pseudotypes were comparable (median radiances: VSVind.G, 1.23×10^8 p/s/cm^2/sr; COCV.G, 3.67×10^7 p/s/cm^2/sr; MARAV.G, 3.73×10^7 p/s/cm^2/sr; and PIRYV.G, 5.01×10^7 p/s/cm^2/sr). These levels remained comparable for all pseudotypes throughout 7 days, indicating that satisfactory gene delivery can be achieved with all envelopes (Figure 4C).

On the other hand, LV challenges of Gth-immunized mice revealed intriguing differences regarding VesGs' capacity to evade the humoral immune response. Although radiances of IC mice challenged with COCV.G-LV and MARAV.G-LV were reduced compared to the CO mice, it was substantially higher than that of VSVind.G-LV (>100-fold on days 2–5), which was again blocked entirely. The weak cross-neutralization we observed against COCV.G and MARAV.G *in vitro* (Figure 3B) translated into a stronger *in vivo* neutralization of the transducing potential of these pseudotypes. MARAV.G-LV's gene delivery efficacy was transient, as bioluminescence levels dropped considerably by day 7. On the other hand, sustained FLuc expression with COCV.G-LV in the IC group was achieved at comparable levels to the CO group and approximately 100-fold higher than IC-VSVind.G. Strikingly PIRYV.G-LV efficacy was unaffected throughout, and significantly higher levels of transgene expression were achieved ($p < 0.0001$ on days 2 and 5, $p < 0.01$ on day 7) (Figure 4D).

These data demonstrated that PIRYV.G-LV outperformed the other pseudotypes, completely evading the neutralizing anti-VSVind.G antibody response. While COCV.G-LV transduction was partially blocked, viable levels of transgene expression were detected and immune evasion could be bolstered with a higher dose.

PIRYV.G-LV Infection Results in Similar Biodistribution Despite Different Receptor Usage

In the CO group of VesG-LV challenge studies, all four pseudotypes demonstrated similar tissue distribution based on the bioluminescence signals observed (Figure 4B). Furthermore, the level of established transgene expression *in vivo* was within 3-fold for all four pseudotypes. The four VesGs investigated throughout this work have varying degrees of sequence homology on the amino acid level (>40% and >70% for VSVind.G, MARAV.G, and COCV.G) (Figure S2), and they are phylogenetically and serologically related. Therefore, we hypothesized that these G proteins may share similar tissue tropism through their receptor usage.

VSVind.G's primary receptor has been identified as the low-density lipoprotein receptor (LDLR).[26,27] To this end, we first evaluated the interaction between soluble recombinant LDLR (sLDLR) and G proteins expressed on the surface of HEK293T cells. As in neutralization assays, RDpro envelope was utilized as a negative control, since its primary receptor has been identified as ASCT-2, a neutral amino acid transporter.[28,29] While COCV.G and MARAV.G bound to sLDLR (Figure 5A), PIRYV.G, like the unrelated RDpro, did not interact with the recombinant receptor protein. Recently, Nikolic and colleagues[27] demonstrated that, while VSVind.G has evolved to interact with cysteine-rich domains of LDLR and other LDLR family members, another vesiculovirus G protein from Chandipura virus does not utilize this receptor. Here we demonstrate that while close phylogenetic relatives of VSVind.G, MARAV.G and COCV.G, share its receptor usage, the more distant PIRYV.G does not. The phylogenetic closeness of PIRYV.G and Chandipura G[20] implies that vesiculoviruses might be split into at least two groups regarding their primary receptor for cell entry.

This discrepancy in binding was further explored through an infection inhibition assay, in which HEK293T cells were challenged with LVs at two MOIs in the presence and absence of sLDLR. Like the binding profiles, PIRYV.G-LV and RDpro-LV infections were unaffected by the presence of sLDLR in the media (Figure 5B). On the other hand, other VesG-LV infections were blocked in a dose-dependent manner, with on average 90% infecton inhibition achieved

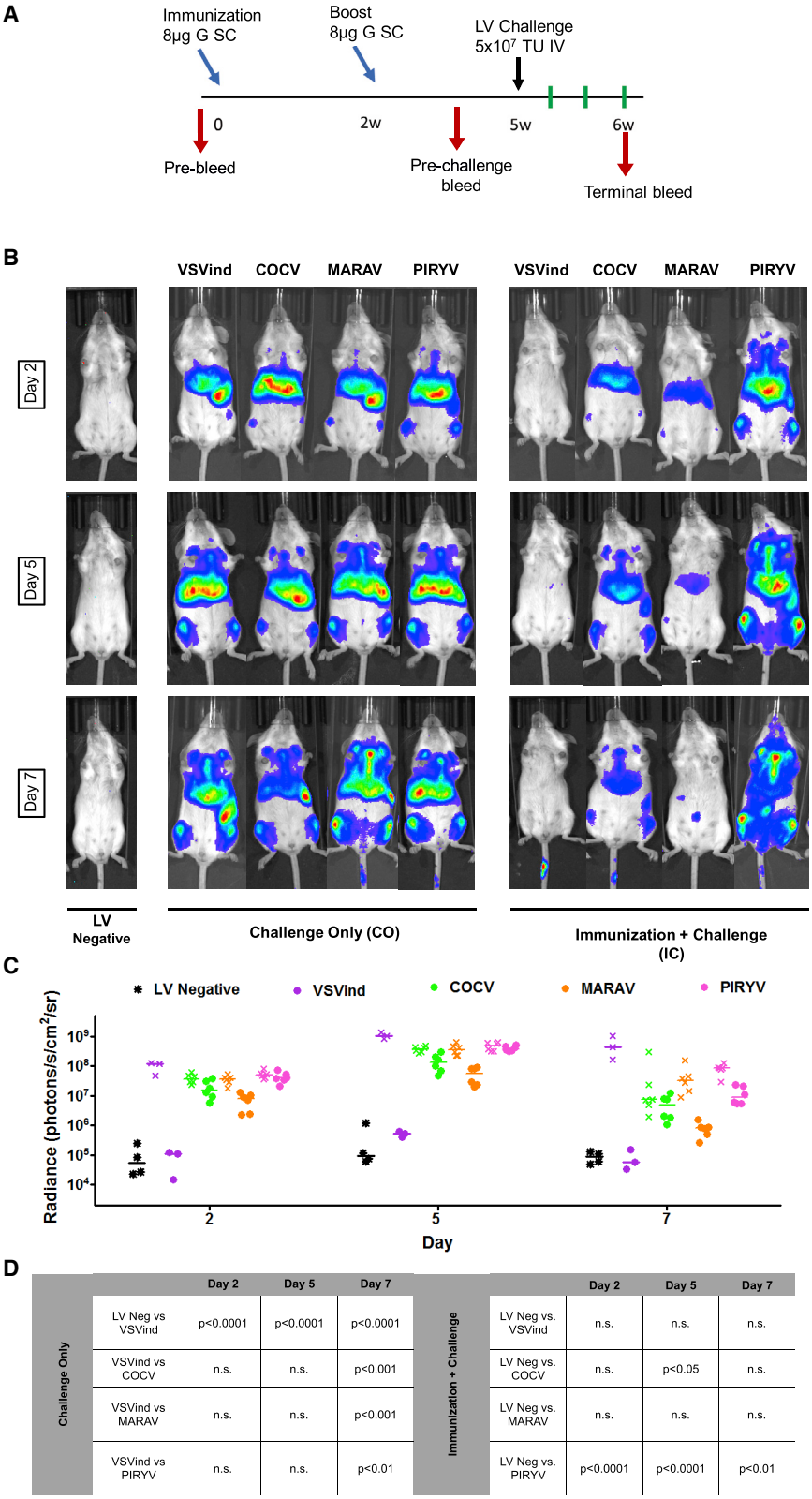

Challenge Only	Day 2	Day 5	Day 7
LV Neg vs VSVind	p<0.0001	p<0.0001	p<0.0001
VSVind vs COCV	n.s.	n.s.	p<0.001
VSVind vs MARAV	n.s.	n.s.	p<0.001
VSVind vs PIRYV	n.s.	n.s.	p<0.01

Immunization + Challenge	Day 2	Day 5	Day 7
LV Neg vs. VSVind	n.s.	n.s.	n.s.
LV Neg vs. COCV	n.s.	p<0.05	n.s.
LV Neg vs. MARAV	n.s.	n.s.	n.s.
LV Neg vs. PIRYV	p<0.0001	p<0.0001	p<0.01

Figure 4. Circumventing Pre-existing Anti-VSVind.G Immunity by Using Other VesGs

(A) Timeline of the study. Immunization and boost points are identified by light blue arrows, while the black arrow indicates the time of LV challenge. Red arrows designate the times at which blood samples were acquired through tail vein bleeds. Green lines show the days on which mice were imaged. At termination of the study, terminal bleeds and post-mortem organ harvest were performed. w, weeks. (B) Representative bioluminescence images of transduced and naive mice at the three time points of days 2, 5, and 7 post-challenge. Localization and the intensity of the luciferase signal are depicted in a heat-map. The envelopes of the challenge vector are indicated at the top of the images, and the experimental groups are located at the bottom. The time points when the images were acquired are indicated on the left. (C) Photon emission from each mouse was quantified as radiance (p/s/cm^2/sr) post-imaging, using region of interest analysis in Living Image software. Each data point represents a mouse and the horizontal bar shows the median. Different colors indicate the pseudotype of the challenge vector; solid dots stand for the IC group and crosses stand for the CO group. (D) Two-way ANOVA followed by Bonferroni multiple comparison test was performed to compare relative radiance levels in CO and IC groups. Comparisons are summarized in a table. Neg, negative; n.s., not significant.

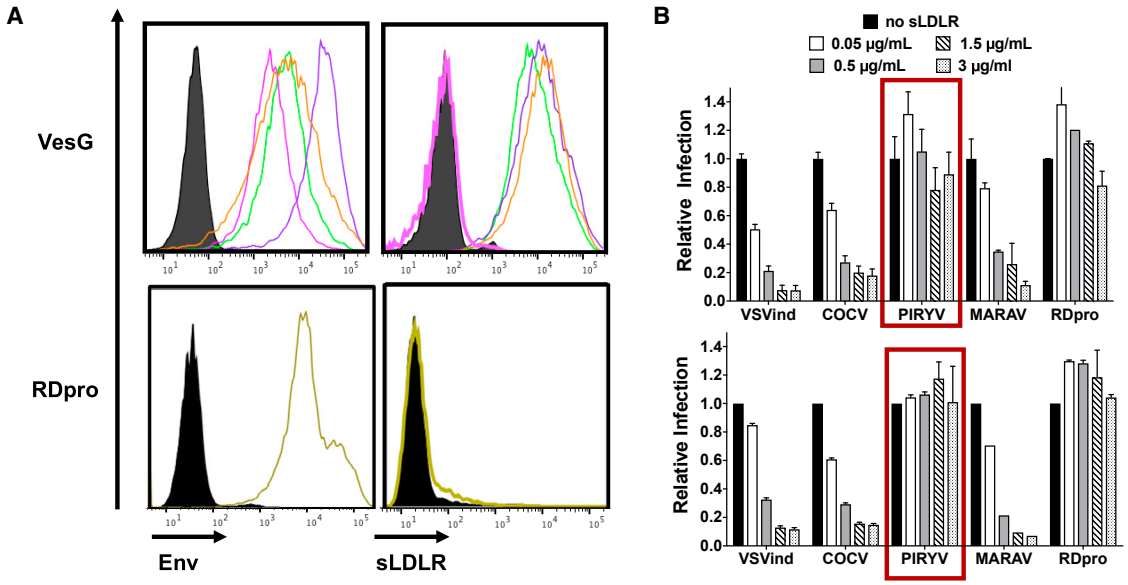

Figure 5. PIRYV.G Does Not Interact with sLDLR

(A) VesG- and RDpro-expressing HEK293T cells were incubated with (left) VSV-Poly and anti-RD114 antiserum to determine envelope expression and (right) sLDLR in parallel. The cells were then probed with the respective secondary antibodies to determine envelope expression and anti-6XHis-tag antibody for sLDLR binding. PIRYV.G did not bind to sLDLR, while the other VesGs demonstrated similar levels of interaction with the soluble receptor protein (the maximum difference between the calculated mean fluorescence intensity [MFI] values was <3-fold). Data shown are one of the three repeats performed. Black, mock; purple, VSVind.G; green, COCV.G; orange, MARAV.G; pink, PIRYV.G; yellow, RDpro. (B) HEK293T cells were challenged with GFP expressing VesG- and RDpro-pseudotyped LVs at MOIs (top) 0.1 and (bottom) 0.5 in the absence and presence of sLDLR. The infection rates were analyzed 48 h later via flow cytometry, and they were normalized to that of sLDLR-free samples. The percentages of GFP of sLDLR-free samples were 2%–10% and 13%–30% for MOIs 0.1 and 0.5, respectively. Data shown represent relative infection ± SD from three experiments performed in duplicates.

with 3 µg/mL sLDLR. The infection hindrance observed, or lack thereof in the case of PIRYV.G, suggested that, while MARAV.G and COCV.G share LDLR as their main receptor with VSVind.G, PIRYV.G does not.

VesG Immunogenicity and the Development of Anti-VesG Immune Response

The investigation of immune response development in response to VesG-LV challenge provided essential insights on VesG immunogenicity. For this analysis, *in vitro* neutralization assays were carried out, and neutralizing activity was determined by normalizing CO and IC group responses to that of control group (i.e., non-immunized, non-challenged) (Figure 6).

Pooled sera from CO mice challenged with COCV.G-LV (CO-COCV.G) and MARAV.G-LV (CO-MARAV.G) demonstrated neutralizing activities against their respective pseudotypes (Figures 6A and 6B). The IC_{50} values for both neutralization profiles were comparable, implying similar levels of immunogenicity (Figure 6G). Interestingly, while the response against COCV.G-LV was specific, MARAV.G-LV administration yielded cross-neutralizing antibodies against VSVind.G, once again indicating homology between immunodominant neutralizing epitopes between these two closely related G proteins. On the other hand, surprisingly, CO-PIRYV.G did not hinder PIRYV.G-LV infectivity (Figure 6C).

Furthermore, the presence of anti-VSVind.G antibodies at the time of the LV challenge boosted the homologous neutralizing anti-VesG response against all pseudotypes (Figure 6D). While IC_{50} values of COCV.G and MARAV.G decreased by approximately 2- and 4-fold, respectively, PIRYV.G-LV infection was partially hindered (<50%). The induction of PIRYV.G-LV-neutralizing response was confirmed by the level of anti-PIRYV.G antibodies in CO and IC sera (Figure 6F).

A similar trend was evident for the neutralizing anti-VSVind.G response. All VesG-LV challenges but PIRYV.G-LV boosted the pre-existing immunity, resulting in a stronger VSVind.G-LV neutralization (Figure 6E). While VSVind.G challenge had the most potent effect, enhancing the neutralizing response by approximately 100-fold, both COCV.G and MARAV.G-LV administrations resulted in the production of cross-neutralizing antibodies and a modest improvement on pre-existing G immunity.

DISCUSSION

In this study, we have explored anti-vector immunity and potential approaches to circumvent the negative effect of this on viral

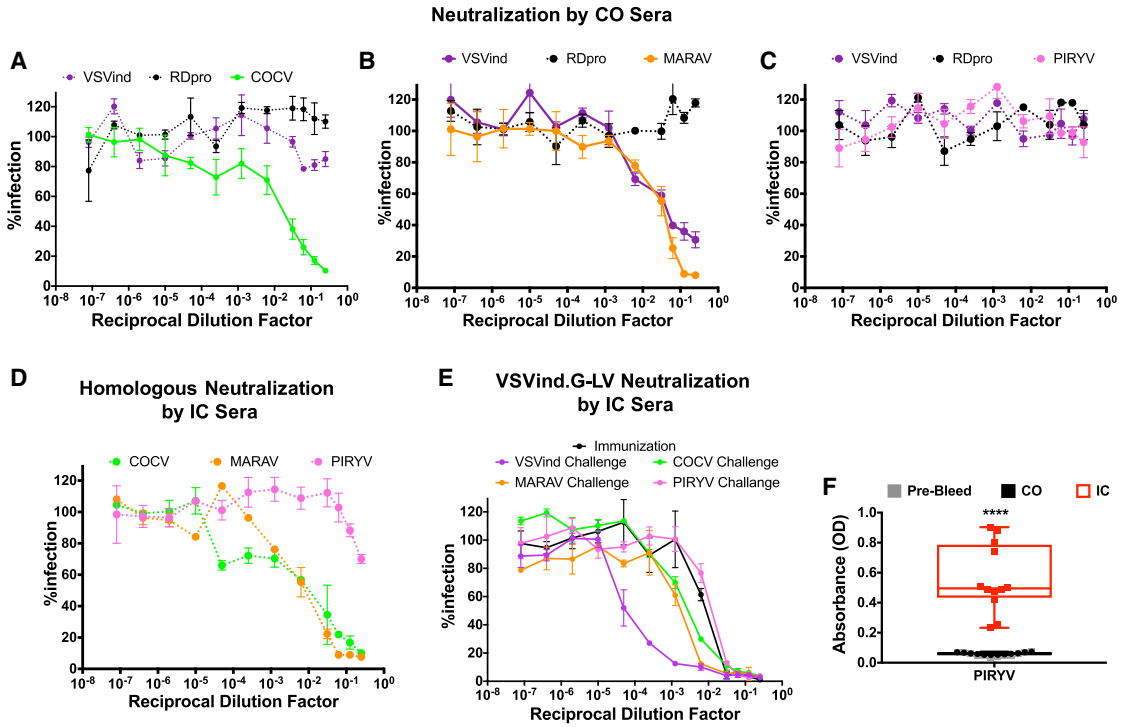

G

Pooled Sera	VesG-LV	IC50 (Reciprocal Dilution Factor)
CO-COCV.G	COCV	1.68 x10^{-2}
	VSVind	no effect
CO-MARAV.G	MARAV	3.09 x10^{-2}
	VSVind	5.15 x10^{-2}
CO-PIRYV.G	PIRYV	no effect
	VSVind	no effect
IC-COCV.G	COCV	1.07 x10^{-2}
IC-MARAV.G	MARAV	8.03 x10^{-3}
IC-PIRYV.G	PIRYV	>4

Figure 6. Neutralizing Antibody Response after VesG-LV Administration

Neutralizing activities of (A) CO-COCV.G, (B) CO-MARAV.G, and (C) CO-PIRYV.G sera isolated from terminal bleeds. (D) Neutralizing activity of IC-COCV.G, IC-MARAV.G, and IC-PIRYV.G sera isolated from terminal bleeds against their respective pseudotypes. (E) Neutralizing activity of IC-VesG sera isolated from terminal bleeds against VSVind.G-LV compared to the neutralizing activity observed after s.c. Gth immunization. Solid lines signify the neutralization effect observed, while the dotted lines indicate the lack of neutralization. The calculated IC_{50} values were as follows: immunization only, 7.15×10^{-3}; COCV, 5.21×10^{-3}; MARAV, 2.49×10^{-3}; PIRYV, 1.90×10^{-2}; and VSVind, 1.52×10^{-4}. Data shown represent the mean ± SD of three repeats performed in duplicates. (F) Anti-PIRYV.G antibodies produced following PIRYV.G-LV challenge of non-immunized (CO) and pre-immunized (IC) mice. One-way ANOVA followed by Tukey's multiple comparison post-test was performed to analyze the significance of the amount of anti-PIRYV.G antibodies produced (****$p < 0.0001$). Data shown represent mean ± SD from two experiments performed in duplicates. (G) Table summarizing measured IC_{50} values of the observed neutralizing activity of CO- and IC-VesG sera. All neutralization experiments were performed as outlined in the Materials and Methods following sera adsorption to HEK293T cells. To calculate IC_{50} values, curves were fitted using the software GraphPad Prism 5 modeled as an [inhibitor] versus response curve with variable hill slopes.

vector-based therapeutic paradigms in the context of LVs. We have demonstrated that i.v. injection of VSVind.G-LVs into naive mice induces a potent and specific neutralizing response (Figure 1). Interestingly, challenging naive mice also revealed a potent anti-HEK293T response, which blocked infection of LVs pseudotyped with the unrelated RDpro envelope *in vitro*. This is thought to be mainly mediated by antibodies that recognize antigens acquired by the vectors during production (e.g., MHC-I). This underlined a major obstacle in studying repeated administration of viral vectors to non-immune-privileged sites in animal models. In addition, the generation of such allo-antibodies may lead to cytotoxicity and allogeneic immune responses in both *in vivo* and *ex vivo* gene therapies in patients.[17,21] These data underscore the importance of stringent quality control criteria with respect to host cell protein

levels in viral vectors destined for clinical development and biological therapies in general.

It has been hypothesized that the induction of a primary immune response, although it wouldn't affect the initial vector injection, could be problematic for subsequent administrations.[1,16,18] Here we have demonstrated the potency of a pre-existing anti-envelope immunity. VSVind.G-LV gene delivery efficacy was significantly reduced to the point of complete abrogation (Figure 2). However, utilizing a phylogenetically distant relative of VSVind.G, PIRYV.G, we were able to demonstrate repeated administration is achievable (Figure 4). In addition, while the efficacy of MARAV.G-LVs was substantially reduced, COCV.G-LVs were partially neutralized but achieved sustained transgene delivery, which may be boosted to higher levels with increased dosage.

The degree of immune evasion achieved by the three different pseudotypes could be explained with regard to phylogenetic relatedness. MARAV.G and COCV.G are two of the closest relatives of VSVind.G, with 78% and 72% homology on the amino acid level, respectively (Figure S2).[20] *In vitro* neutralization assays performed using the sera isolated from terminal bleeds of IC-VSVind.G displayed weak but neutralizing cross-reactivity against these two pseudotypes (Figure 3). This implied that these three closely related G proteins share immunodominant epitopes, which neutralizing antibodies recognize. Furthermore, they may also share several other immunogenic determinants, which are recognized by non-neutralizing antibodies. These antibodies most probably contribute to concerted efforts of the immune system through several mechanisms: coating the viral vectors and leading to vector aggregation, aiding deposition of complement cascade proteins leading to vector opsonization, and contributing to antigen presentation stimulating the activation of macrophages and cytotoxic T cells.[30–34] This would explain the more robust viral transduction hindrance observed *in vivo* compared to the modest vector neutralization *in vitro*. On the other hand, PIRYV.G, with only 40% amino acid homology, may lack these determinants, rendering the antibodies unable to bind to the glycoprotein.

In addition, administration of these four different pseudotypes led to distinct humoral immune responses. Following i.v. injection of VesG-LV into naive mice, envelope-specific-neutralizing antibodies were detected for VSVind.G, COCV.G, and MARAV.G, but not for PIRYV.G (Figures 6A–6C). PIRYV.G-LV infection was blocked partially (<50%) only with IC-PIRYV.G sera, while complete neutralization was observed for both CO- and IC-VesG sera for other pseudotypes. Similarly, the administration of VSVind.G-, COCV.G-, and MARAV.G-LVs to pre-immunized mice strengthened the pre-existing anti-VSVind.G immunity, while PIRYV.G-LV injection had no effect (Figure 6E). It can be deduced from the data that PIRYV.G, in comparison to the other three G proteins, may be less immunogenic and might need several more boosts and/or sequential administrations to elicit a robust neutralizing response.

A recent study in which the low pH conformation of another vesiculovirus, Chandipura virus (CHAV), was investigated revealed several evolutionary variances among VesGs.[35] Comparison of the CHAV.G 3D structure and previously elucidated VSVind.G structures highlighted selective pressure of primary immune responses, with regard to the main antigenic sites of the G proteins.[22,23] Therefore, the overall structural differences between PIRYV.G (a closer phylogenetic relative of CHAV.G in comparison to VSVind.G) and the other tested VesGs could lead to substantially different antigen presentation. Therefore, the way antigenic domains are structured may dictate the immunogenicity difference as well as the lack of cross-neutralization observed with pooled mice sera. Another reason behind the lack of neutralizing PIRYV.G-LV antibodies may be the number of glycoprotein spikes acquired by LVs during assembly and budding from the producer cells. PIRYV.G-LVs may have a considerably smaller number of glycoproteins compared to the other VesG-LVs, therefore providing the immune system with fewer immunogenic targets and leading to a weaker response.

Transgene delivery levels in the CO group mice, in both studies, provided insights on *in vivo* effectiveness of complement-mediated viral vector inactivation. Serum sensitivity of wild-type (WT) VSVind and VSVind.G-LV is well established in the literature.[30,36–40] We have previously reported that COCV.G, MARAV.G, and PIRYV.G are substantially more resistant to complement-mediated inactivation by both human and mouse sera.[25] Recent studies have demonstrated the dose-dependent nature of complement-mediated LV inactivation.[3,21,41] It has been suggested that the titers utilized *in vivo* are high enough to saturate this neutralizing response. *In vivo* bioluminescence imaging (Figure 4B) and luciferase activity detected in organs (data not shown) harvested post-mortem have confirmed this. VSVind.G-LV transduction efficiency was comparable to that achieved with serum-resistant pseudotypes. This highlights that *in vivo* transduction efficiency may have not been hindered substantially by the complement system in this experimental setting. Furthermore, while a similar overall biodistribution was observed for all four pseudotypes (Figure 4B; post-mortem organ bioluminescence data not shown), a closer investigation revealed that they do not utilize the same receptor as their major cellular entryway (Figure 5). This may alter the types of cells transduced within a tissue, and, therefore, it may affect any further anti-transgene immune responses and, hence, long-term transgene expression levels.

In the past, translation from animal models to clinical settings for gene therapy has not always been straightforward. However, taken together, this study serves as the proof of principle for a vector administration method in gene therapy, and it has some implication also for oncolytic virotherapy. Recombinant versions of the VSV backbone have shown significant potential for cancer immunotherapy.[42,43] Human infections with VSVind are very rare and isolated to regions where VSVind is endemic. Seroprevalance in the human population is, therefore, likely to be low, with the general population largely free of pre-existing neutralizing antibodies.[44] Thus, we speculate the pseudotyping approaches outlined in this report could be applied to allow repeated injections over more protracted time frames. Furthermore, it is possible

that VSV pseudotyped with these unconventional G proteins may have improved tumor targeting, specificity, and replicative capacity; but, this is purely speculative at this stage. However, we do believe this method will allow tailoring a panel of pseudotypes for every individual, as well as improved potential for repeated systemic administration of vectors and viruses to achieve sustained therapeutic levels of transgene expression and anti-tumor effects.

MATERIALS AND METHODS

Cell Culture

In all experiments, HEK293T cells were used. The cell line was maintained in DMEM (Sigma-Aldrich, St. Louis, MO, USA), supplemented with 10% heat-inactivated fetal calf serum (Gibco, Carlsbad, CA, USA), 2 mM L-Glutamine (Gibco), 100 U/mL penicillin (Gibco), and 100 μg/mL streptomycin (Gibco). Cells were kept in cell culture incubators at 37°C and 5% CO_2.

LV Preparation

Three-plasmid co-transfection into HEK293T cells was used to make pseudotyped LV, as described previously.[45] Briefly, 2×10^7 cells were seeded in 15-cm plates. Then 24 h later, they were transfected using FuGene6 (Promega, Madison, WI, USA) with the following plasmids: 3.75 μg pCCL.Fluc.2A.EGFP (firefly luciferase and EGFP-expressing vector plasmid),[46] 2.5 μg p8.91 (Gag-Pol and Rev expression plasmid),[45] and 2.5 μg VesG expression plasmids previously described.[20,25] Then 4 h after transfection, medium was changed to OptiMEM (Gibco), supplemented with 2 mM L-Glutamine (Gibco), 100 U/mL penicillin (Gibco), and 100 μg/mL streptomycin (Gibco). Vector-containing media were collected 48 and 72 h after transfection, pooled, passed through Whatman Puradisc 0.45-μm cellulose acetate filters (SLS, UK), and concentrated ~100-fold by ultra-centrifugation at 22,000 rpm (87,119 × *g*) for 2 h at 4°C in Beckmann Optima LK-90 ultracentrifuge using the SW-28 swinging bucket rotor. Titers of vectors were estimated on HEK293T cells via flow cytometry and qPCR measuring proviral copies, as previously described.[20,25] For all concentrated VesG-pseudotyped vectors, titers ranged from 0.6 to 1.1 × 10^9 TU/mL (Figure S1).

Mice

All animal studies described were done according to protocols approved by Biological Services Division (BSD) at the National Institute for Biological Standards and Control (NIBSC) and within the remit of a Home Office Project License (PPL 70/8091). Animals were purchased from Charles River Laboratories (Kent, UK). The 6- to 8-week-old female BALB/c mice with a minimum weight of 18 g were used for both experiments. Mice were immunized and boosted with wild-type VSVind.G protein produced by thermolysin-limited proteolysis of viral particles (Gth),[22,23] subcutaneously using the Sigma Adjuvant System (Sigma-Aldrich) at 0.08 mg/mL antigen concentration. LVs were administered i.v. into the tail vein.

Blood sampling was performed by tail vein bleeding. Serum was obtained by centrifuging clotted blood samples at 10,000 × *g* for 15 min at 4°C. Serum was stored at −20°C until further use.

In Vivo Bioluminescence Imaging

Transduction efficacy, transgene expression, and biodistribution of the viral vectors were monitored using the IVIS Spectrum *In Vivo* Imaging System (PerkinElmer, Waltham, MA, USA). Mice were injected intraperitoneally with D-Luciferin (PerkinElmer) in PBS at a 150 mg/kg body weight dose prior to subjection to general anesthesia via isoflurane inhalation in the induction chamber. Mice were then transferred to the imaging chamber while anesthesia was maintained, and images were captured between 10 and 15 min post D-Luciferin injection. Mice were monitored during recovery after imaging. Images were analyzed, and radiance was determined via region of interest (ROI) analysis using Living Image software (PerkinElmer).

Serum Neutralization Assay

To determine the presence of neutralizing antibodies in murine sera and the strength of the neutralizing immune response induced, an infection assay was performed. Briefly, HEK293T cells were seeded in a 96-well plate at a density of 2×10^4 cells/well with 200 μL medium containing 8 μg/mL polybrene. For all neutralization experiments except for the one shown in Figure 1, pooled serum samples were first adsorbed to HEK293T cells: prior to incubating with LVs, sera were pooled and incubated with 1×10^7 HEK293T cells/150 μL sera on ice for 1 h. Following, adsorbed sera were serially diluted in plain OptiMEM to 12 different concentrations ranging from 1:2 dilution to 1:6,250,000 dilution. Of each serum dilution, 10 μL was mixed 1:1 v/v with the indicated LV pseudotypes at 4.0×10^5 TU/mL titer, incubated at 37°C for 1 h, and plated on the cells. At 48 h after challenging the cells with the serum-LV mixes, cells were trypsinized and analyzed for GFP expression by flow cytometry. Measured titers were normalized to that obtained after mixing the LVs with dilutions of sera collected from control mice (i.e., non-immunized and non-challenged), using the following equation:

$$\text{Infection } \% = \frac{\text{Titer of LV incubated with experimental sera}}{\text{Titer of LV incubated with control sera}} \times 100.$$

The data obtained from the above analysis were plotted against antiserum dilutions using the graphing and statistics software GraphPad Prism 5. Furthermore, non-linear regression analysis was carried out using the same software to fit neutralization ([inhibitor] versus response) curves and calculate IC_{50} values (Figure S3).

Infection Assay to Evaluate the Role of LDLR in Lentiviral Entry

To determine whether the human LDLR plays a role in mediating infection of pseudotyped LVs, an infection assay was performed in the presence and absence of sLDLR. HEK293T cells were seeded at a density of 2×10^4 cells/well in 96-well plates in 100 μL complete medium. Then 3 h later, these cells were incubated, for 30 min at 37°C, with four different concentrations of sLDLR (0.05, 0.5, 1.5, and 3 μg/mL) (R&D Systems, Minneapolis, MN, USA). The cells were then challenged with GFP encoding VesG- or RDpro-pseudotyped LVs at two MOIs (0.1 or 0.5) in a total volume of 120 μL.

Then 48 h later, transduced cells were analyzed for GFP expression by flow cytometry.

sLDLR Binding to G Protein-Expressing Cells

Cells were transfected with VesG and RDpro expression plasmids[20,25] by lipofection using FuGENE6 (Promega, Madison, WI, USA). Cells were plated in U-bottom 96-well plates at equal densities. Cells were then incubated with the extracellular polyclonal VSV-Poly[20] or anti-RD114 antiserum (NCI, Rockville, MD, USA) at 1:200 or 1:500 dilution, respectively, or 3 μg/mL sLDLR in 1% BSA in PBS in a total reaction volume of 100 μL. After washing twice with PBS, cells stained with anti-VSVind.G and anti-RDpro antibodies were incubated with their respective secondary antibodies. On the other hand, the cells incubated with sLDLR were stained with an anti-6XHis-tag antibody, ab18184 (Abcam, UK), against the C-terminal 6XHis-tag on sLDLR to probe for sLDLR binding. Cells were then washed twice with PBS, fixed in 2% paraformaldehyde (PFA) in PBS, and analyzed via flow cytometry.

LV-Based ELISA

An ELISA was used to detect anti-VesG antibodies in murine sera. For this, LVs pseudotyped with different VesGs and with no envelope (ΔEnv) were produced as previously described. Total protein concentrations of the LV preparations were determined using a Pierce BCA Protein Assay Kit, according to the manufacturer's instructions, using BSA as the standard. A coating mix of 25 μg/mL total protein in PBS was prepared, and each well of Nunc Maxisorp ELISA plate (Thermo Fisher Scientific, UK) was coated at a volume of 100 μL/well overnight at 4°C. The plate was washed three times with 200 μL PBS before the samples were incubated with 200 μL/well blocking buffer and 2% fish gelatine (Sigma-Aldrich) in PBS, for 1 h at 37°C. The plate was washed three times with 300 μL/well washing buffer, PBS-0.05% (v/v) Tween20, before 100 μL/well serum samples diluted in diluent buffer, 10% fetal calf serum (FCS) (heat inactivated) in PBS, were added to the wells and incubated at 37°C for 2 h. After another three washes, the samples were incubated with the secondary antibody, horseradish peroxidase (HRP)-conjugated anti-mouse IgG (Jackson ImmunoResearch Laboratories) diluted 1:1,000 in diluent buffer for 1 h at 37°C. Following three washes, 100 μL/well Ultra TMB-ELISA Substrate (Thermo Fisher Scientific) was added to each well incubated at room temperature for 10 min, and the reaction was stopped by adding an isovolume of 1 M sulfuric acid. The absorbance was determined at 450 nm using a FluoStar Omega Plate Reader (BMG Labtech).

Ig-Isotyping ELISA

Ig-Isotyping Mouse Uncoated ELISA kit (Thermo Scientific) was used to perform the analysis. Wells in a Nunc Maxisorp 96-well plate (Thermo Scientific) were coated overnight at 4°C with 50 ng/well in PBS recombinant VSVind.G protein (Source Bioscience). Following blocking, pooled serum samples were added at 1:100 in the diluent buffer provided and incubated for 1 h at room temperature. Following incubation for 1 h with rat anti-mouse Ig antibodies provided and diluted 1:100 in diluent buffer, HRP-conjugated anti-rat IgG (Jackson ImmunoResearch Laboratories) was used to determine the antibody signal. Absorbance was read using a FluoStar Omega Plate Reader (BMG Labtech).

Statistical Analyses

All statistical analyses were performed using the GraphPad Prism 5 software (GraphPad, La Jolla, CA, USA). Details of all tests, including the calculated p values, are indicated in the respective figure legends.

SUPPLEMENTAL INFORMATION

Supplemental Information can be found online at https://doi.org/10.1016/j.omtn.2019.05.010.

AUTHOR CONTRIBUTIONS

A.M.M. designed and performed experiments to obtain the presented data and wrote the paper. G.M. performed experiments and helped interpreting data. E.M.B. performed experiments. M.K.C. helped designing experiments and interpreting data. J.E.E. and Y.T. supervised the study and wrote the paper.

ACKNOWLEDGMENTS

We would like to acknowledge Dr. Maha Tijani for her constructive discussions and shared reagents. We would like to thank Drs. Yves Gaudin and Aurélie Albertini for the Gth protein and the Biological Services Division at the National Institute of Biological Standards and Control for their expertise and help in parts of this study. A.M.M.'s studentship is funded by NIBSC.

REFERENCES

1. Nayak, S., and Herzog, R.W. (2010). Progress and prospects: immune responses to viral vectors. Gene Ther. *17*, 295–304.

2. Palfi, S., Gurruchaga, J.M., Ralph, G.S., Lepetit, H., Lavisse, S., Buttery, P.C., Watts, C., Miskin, J., Kelleher, M., Deeley, S., et al. (2014). Long-term safety and tolerability of ProSavin, a lentiviral vector-based gene therapy for Parkinson's disease: a dose escalation, open-label, phase 1/2 trial. Lancet *383*, 1138–1146.

3. Cantore, A., Ranzani, M., Bartholomae, C.C., Volpin, M., Valle, P.D., Sanvito, F., Sergi, L.S., Gallina, P., Benedicenti, F., Bellinger, D., et al. (2015). Liver-directed lentiviral gene therapy in a dog model of hemophilia B. Sci. Transl. Med. *7*, 277ra28.

4. Meneghini, V., Lattanzi, A., Tiradani, L., Bravo, G., Morena, F., Sanvito, F., Calabria, A., Bringas, J., Fisher-Perkins, J.M., Dufour, J.P., et al. (2016). Pervasive supply of therapeutic lysosomal enzymes in the CNS of normal and Krabbe-affected non-human primates by intracerebral lentiviral gene therapy. EMBO Mol. Med. *8*, 489–510.

5. Alton, E.W., Beekman, J.M., Boyd, A.C., Brand, J., Carlon, M.S., Connolly, M.M., Chan, M., Conlon, S., Davidson, H.E., Davies, J.C., et al. (2017). Preparation for a first-in-man lentivirus trial in patients with cystic fibrosis. Thorax *72*, 137–147.

6. Cartier, N., Hacein-Bey-Abina, S., Bartholomae, C.C., Veres, G., Schmidt, M., Kutschera, I., Vidaud, M., Abel, U., Dal-Cortivo, L., Caccavelli, L., et al. (2009). Hematopoietic stem cell gene therapy with a lentiviral vector in X-linked adrenoleukodystrophy. Science *326*, 818–823.

7. Cavazzana-Calvo, M., Payen, E., Negre, O., Wang, G., Hehir, K., Fusil, F., Down, J., Denaro, M., Brady, T., Westerman, K., et al. (2010). Transfusion independence and HMGA2 activation after gene therapy of human β-thalassaemia. Nature *467*, 318–322.

8. Aiuti, A., Biasco, L., Scaramuzza, S., Ferrua, F., Cicalese, M.P., Baricordi, C., Dionisio, F., Calabria, A., Giannelli, S., Castiello, M.C., et al. (2013). Lentiviral hematopoietic stem cell gene therapy in patients with Wiskott-Aldrich syndrome. Science *341*, 1233151.

9. Sessa, M., Lorioli, L., Fumagalli, F., Acquati, S., Redaelli, D., Baldoli, C., Canale, S., Lopez, I.D., Morena, F., Calabria, A., et al. (2016). Lentiviral haemopoietic stem-cell gene therapy in early-onset metachromatic leukodystrophy: an ad-hoc analysis of a non-randomised, open-label, phase 1/2 trial. Lancet *388*, 476–487.

10. Ribeil, J.A., Hacein-Bey-Abina, S., Payen, E., Magnani, A., Semeraro, M., Magrin, E., Caccavelli, L., Neven, B., Bourget, P., El Nemer, W., et al. (2017). Gene Therapy in a Patient with Sickle Cell Disease. N. Engl. J. Med. *376*, 848–855.

11. Herzog, R.W. (2017). Complexity of immune responses to AAV transgene products - example of factor IX. Cell Immunol. Published online May 29, 2017. https://doi.org/10.1016/j.cellimm.2017.05.006.

12. Power, A.T., Wang, J., Falls, T.J., Paterson, J.M., Parato, K.A., Lichty, B.D., Stojdl, D.F., Forsyth, P.A., Atkins, H., and Bell, J.C. (2007). Carrier cell-based delivery of an oncolytic virus circumvents antiviral immunity. Mol. Ther. *15*, 123–130.

13. Hangartner, L., Zinkernagel, R.M., and Hengartner, H. (2006). Antiviral antibody responses: the two extremes of a wide spectrum. Nat. Rev. Immunol. *6*, 231–243.

14. Abordo-Adesida, E., Follenzi, A., Barcia, C., Sciascia, S., Castro, M.G., Naldini, L., and Lowenstein, P.R. (2005). Stability of lentiviral vector-mediated transgene expression in the brain in the presence of systemic antivector immune responses. Hum. Gene Ther. *16*, 741–751.

15. Maguire, C.A., Ramirez, S.H., Merkel, S.F., Sena-Esteves, M., and Breakefield, X.O. (2014). Gene therapy for the nervous system: challenges and new strategies. Neurotherapeutics *11*, 817–839.

16. Annoni, A., Goudy, K., Akbarpour, M., Naldini, L., and Roncarolo, M.G. (2013). Immune responses in liver-directed lentiviral gene therapy. Transl. Res. *161*, 230–240.

17. Follenzi, A., Santambrogio, L., and Annoni, A. (2007). Immune responses to lentiviral vectors. Curr. Gene Ther. *7*, 306–315.

18. Annoni, A., Gregori, S., Naldini, L., and Cantore, A. (2018). Modulation of immune responses in lentiviral vector-mediated gene transfer. Cell. Immunol. Published online April 27, 2018. https://doi.org/10.1016/j.cellimm.2018.04.012.

19. Annoni, A., Brown, B.D., Cantore, A., Sergi, L.S., Naldini, L., and Roncarolo, M.G. (2009). In vivo delivery of a microRNA-regulated transgene induces antigen-specific regulatory T cells and promotes immunologic tolerance. Blood *114*, 5152–5161.

20. Munis, A.M., Tijani, M., Hassall, M., Mattiuzzo, G., Collins, M.K., and Takeuchi, Y. (2018). Characterization of Antibody Interactions with the G Protein of Vesicular Stomatitis Virus Indiana Strain and Other Vesiculovirus G Proteins. J. Virol. *92*, e00900-18.

21. Milani, M., Annoni, A., Bartolaccini, S., Biffi, M., Russo, F., Di Tomaso, T., Raimondi, A., Lengler, J., Holmes, M.C., Scheiflinger, F., et al. (2017). Genome editing for scalable production of alloantigen-free lentiviral vectors for *in vivo* gene therapy. EMBO Mol. Med. *9*, 1558–1573.

22. Roche, S., Bressanelli, S., Rey, F.A., and Gaudin, Y. (2006). Crystal structure of the low-pH form of the vesicular stomatitis virus glycoprotein G. Science *313*, 187–191.

23. Roche, S., Rey, F.A., Gaudin, Y., and Bressanelli, S. (2007). Structure of the prefusion form of the vesicular stomatitis virus glycoprotein G. Science *315*, 843–848.

24. Brown, B.D., Sitia, G., Annoni, A., Hauben, E., Sergi, L.S., Zingale, A., Roncarolo, M.G., Guidotti, L.G., and Naldini, L. (2007). In vivo administration of lentiviral vectors triggers a type I interferon response that restricts hepatocyte gene transfer and promotes vector clearance. Blood *109*, 2797–2805.

25. Tijani, M., Munis, A.M., Perry, C., Sanber, K., Ferraresso, M., Mukhopadhyay, T., Themis, M., Nisoli, I., Mattiuzzo, G., Collins, M.K., and Takeuchi, Y. (2018). Lentivector Producer Cell Lines with Stably Expressed Vesiculovirus Envelopes. Mol. Ther. Methods Clin. Dev. *10*, 303–312.

26. Finkelshtein, D., Werman, A., Novick, D., Barak, S., and Rubinstein, M. (2013). LDL receptor and its family members serve as the cellular receptors for vesicular stomatitis virus. Proc. Natl. Acad. Sci. USA *110*, 7306–7311.

27. Nikolic, J., Belot, L., Raux, H., Legrand, P., Gaudin, Y., and A Albertini, A. (2018). Structural basis for the recognition of LDL-receptor family members by VSV glycoprotein. Nat. Commun. *9*, 1029.

28. Rasko, J.E., Battini, J.L., Gottschalk, R.J., Mazo, I., and Miller, A.D. (1999). The RD114/simian type D retrovirus receptor is a neutral amino acid transporter. Proc. Natl. Acad. Sci. USA *96*, 2129–2134.

29. Tailor, C.S., Nouri, A., Zhao, Y., Takeuchi, Y., and Kabat, D. (1999). A sodium-dependent neutral-amino-acid transporter mediates infections of feline and baboon endogenous retroviruses and simian type D retroviruses. J. Virol. *73*, 4470–4474.

30. Tesfay, M.Z., Ammayappan, A., Federspiel, M.J., Barber, G.N., Stojdl, D., Peng, K.W., and Russell, S.J. (2014). Vesiculovirus neutralization by natural IgM and complement. J. Virol. *88*, 6148–6157.

31. La Gruta, N.L., and Turner, S.J. (2014). T cell mediated immunity to influenza: mechanisms of viral control. Trends Immunol. *35*, 396–402.

32. Klasse, P.J. (2014). Neutralization of Virus Infectivity by Antibodies: Old Problems in New Perspectives. Adv. Biol. *2014*, 157895.

33. Klasse, P.J., and Sattentau, Q.J. (2002). Occupancy and mechanism in antibody-mediated neutralization of animal viruses. J. Gen. Virol. *83*, 2091–2108.

34. Klasse, P.J., and Sattentau, Q.J. (2001). Mechanisms of virus neutralization by antibody. Curr. Top. Microbiol. Immunol. *260*, 87–108.

35. Baquero, E., Albertini, A.A., Raux, H., Buonocore, L., Rose, J.K., Bressanelli, S., and Gaudin, Y. (2015). Structure of the low pH conformation of Chandipura virus G reveals important features in the evolution of the vesiculovirus glycoprotein. PLoS Pathog. *11*, e1004756.

36. DePolo, N.J., Reed, J.D., Sheridan, P.L., Townsend, K., Sauter, S.L., Jolly, D.J., and Dubensky, T.W., Jr. (2000). VSV-G pseudotyped lentiviral vector particles produced in human cells are inactivated by human serum. Mol. Ther. *2*, 218–222.

37. Croyle, M.A., Callahan, S.M., Auricchio, A., Schumer, G., Linse, K.D., Wilson, J.M., Brunner, L.J., and Kobinger, G.P. (2004). PEGylation of a vesicular stomatitis virus G pseudotyped lentivirus vector prevents inactivation in serum. J. Virol. *78*, 912–921.

38. Tesfay, M.Z., Kirk, A.C., Hadac, E.M., Griesmann, G.E., Federspiel, M.J., Barber, G.N., Henry, S.M., Peng, K.W., and Russell, S.J. (2013). PEGylation of vesicular stomatitis virus extends virus persistence in blood circulation of passively immunized mice. J. Virol. *87*, 3752–3759.

39. Beebe, D.P., and Cooper, N.R. (1981). Neutralization of vesicular stomatitis virus (VSV) by human complement requires a natural IgM antibody present in human serum. J. Immunol. *126*, 1562–1568.

40. Takeuchi, Y., Liong, S.H., Bieniasz, P.D., Jäger, U., Porter, C.D., Friedman, T., McClure, M.O., and Weiss, R.A. (1997). Sensitization of rhabdo-, lenti-, and spumaviruses to human serum by galactosyl(alpha1-3)galactosylation. J. Virol. *71*, 6174–6178.

41. Cantore, A., Nair, N., Della Valle, P., Di Matteo, M., Màtrai, J., Sanvito, F., Brombin, C., Di Serio, C., D'Angelo, A., Chuah, M., et al. (2012). Hyperfunctional coagulation factor IX improves the efficacy of gene therapy in hemophilic mice. Blood *120*, 4517–4520.

42. Durham, N.M., Mulgrew, K., McGlinchey, K., Monks, N.R., Ji, H., Herbst, R., Suzich, J., Hammond, S.A., and Kelly, E.J. (2017). Oncolytic VSV Primes Differential Responses to Immuno-oncology Therapy. Mol. Ther. *25*, 1917–1932.

43. Bishnoi, S., Tiwari, R., Gupta, S., Byrareddy, S.N., and Nayak, D. (2018). Oncotargeting by Vesicular Stomatitis Virus (VSV): Advances in Cancer Therapy. Viruses *10*, E90.

44. Fuchs, J.D., Frank, I., Elizaga, M.L., Allen, M., Frahm, N., Kochar, N., Li, S., Edupuganti, S., Kalams, S.A., Tomaras, G.D., et al.; HVTN 090 Study Group and the National Institutes of Allergy and Infectious Diseases HIV Vaccine Trials Network (2015). First-in-Human Evaluation of the Safety and Immunogenicity of a Recombinant Vesicular Stomatitis Virus Human Immunodeficiency Virus-1 gag Vaccine (HVTN 090). Open Forum Infect. Dis. *2*, ofv082.

45. Zufferey, R., Nagy, D., Mandel, R.J., Naldini, L., and Trono, D. (1997). Multiply attenuated lentiviral vector achieves efficient gene delivery in vivo. Nat. Biotechnol. *15*, 871–875.

46. Vink, C.A., Counsell, J.R., Perocheau, D.P., Karda, R., Buckley, S.M.K., Brugman, M.H., Galla, M., Schambach, A., McKay, T.R., Waddington, S.N., and Howe, S.J. (2017). Eliminating HIV-1 Packaging Sequences from Lentiviral Vector Proviruses Enhances Safety and Expedites Gene Transfer for Gene Therapy. Mol. Ther. *25*, 1790–1804.

OMTN, Volume *17*

Supplemental Information

Use of Heterologous Vesiculovirus G Proteins Circumvents the Humoral Anti-envelope Immunity in Lentivector-Based *In Vivo* Gene Delivery

Altar M. Munis, Giada Mattiuzzo, Emma M. Bentley, Mary K. Collins, James E. Eyles, and Yasuhiro Takeuchi

SUPPLEMENTARY FIGURES

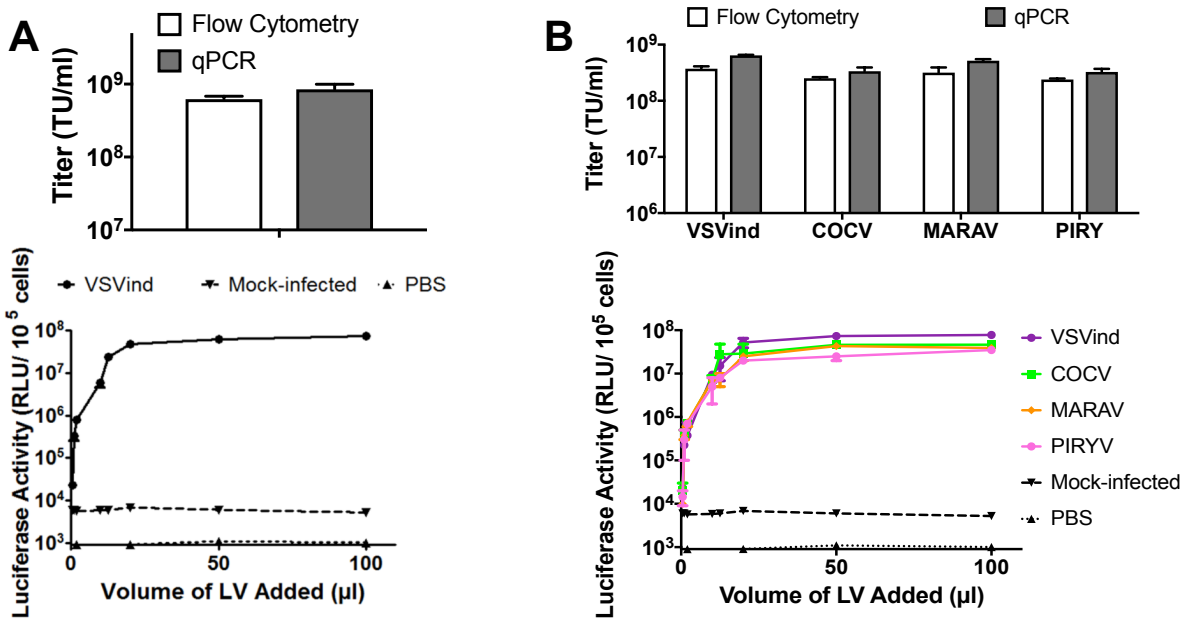

<u>Supplementary Figure S1: Titers and Luciferase Activity of the LVs Used.</u> qPCR and flow cytometry-based titers and luciferase activity of the vectors used in the **(A)** initial VSVind.G-LV challenge and **(B)** VesG-LV challenge studies**.**

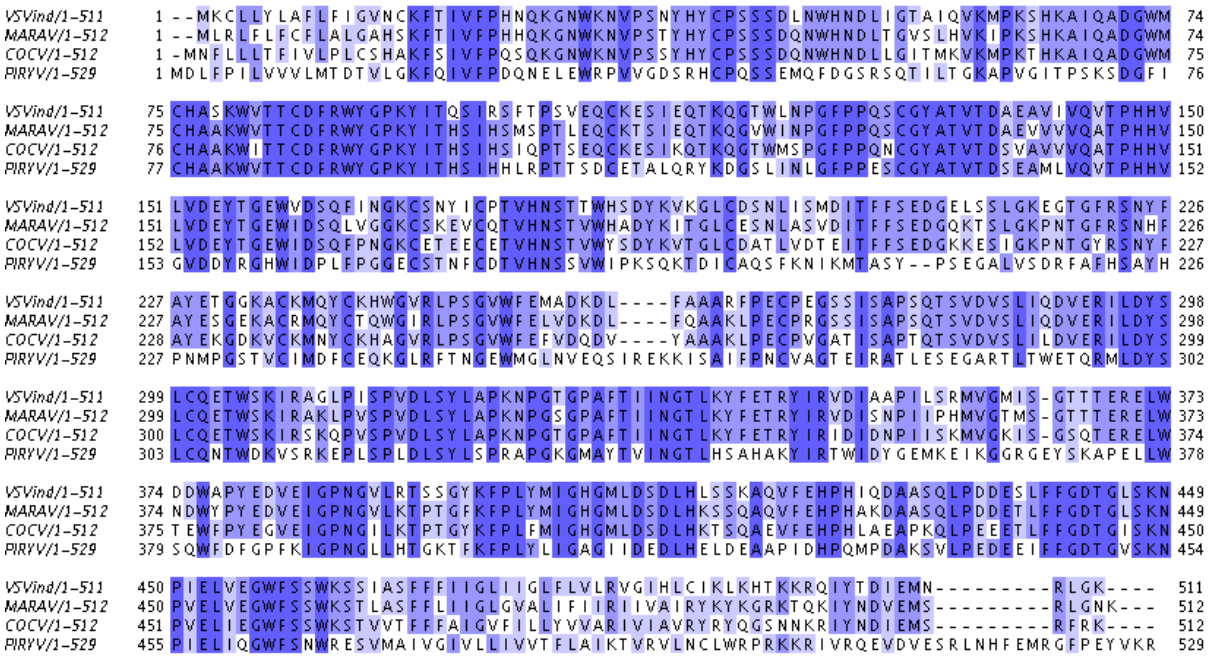

<u>Supplementary Figure S2: Multiple Amino Acid Sequence Alignment of the G proteins of Vesiculoviruses.</u> The sequences of vesiculoviruses (VSVind, UniProt: P03522; MARAV, UniProt: F8SPF4; COCV, UniProt: O56677; PIRYV, UniProt: Q85213) were aligned using ClustalOmega online multiple sequence alignment tool (EMBL-EPI), and the alignments were visualized using JalView software.[1] Dashed lines represent gaps introduced to maximize matching of amino acid residues. Blue shading indicates percent identity; dark blue: 80-100%, medium blue: 60-80% light blue: 40-60%, and no colour indicating <40% identity.

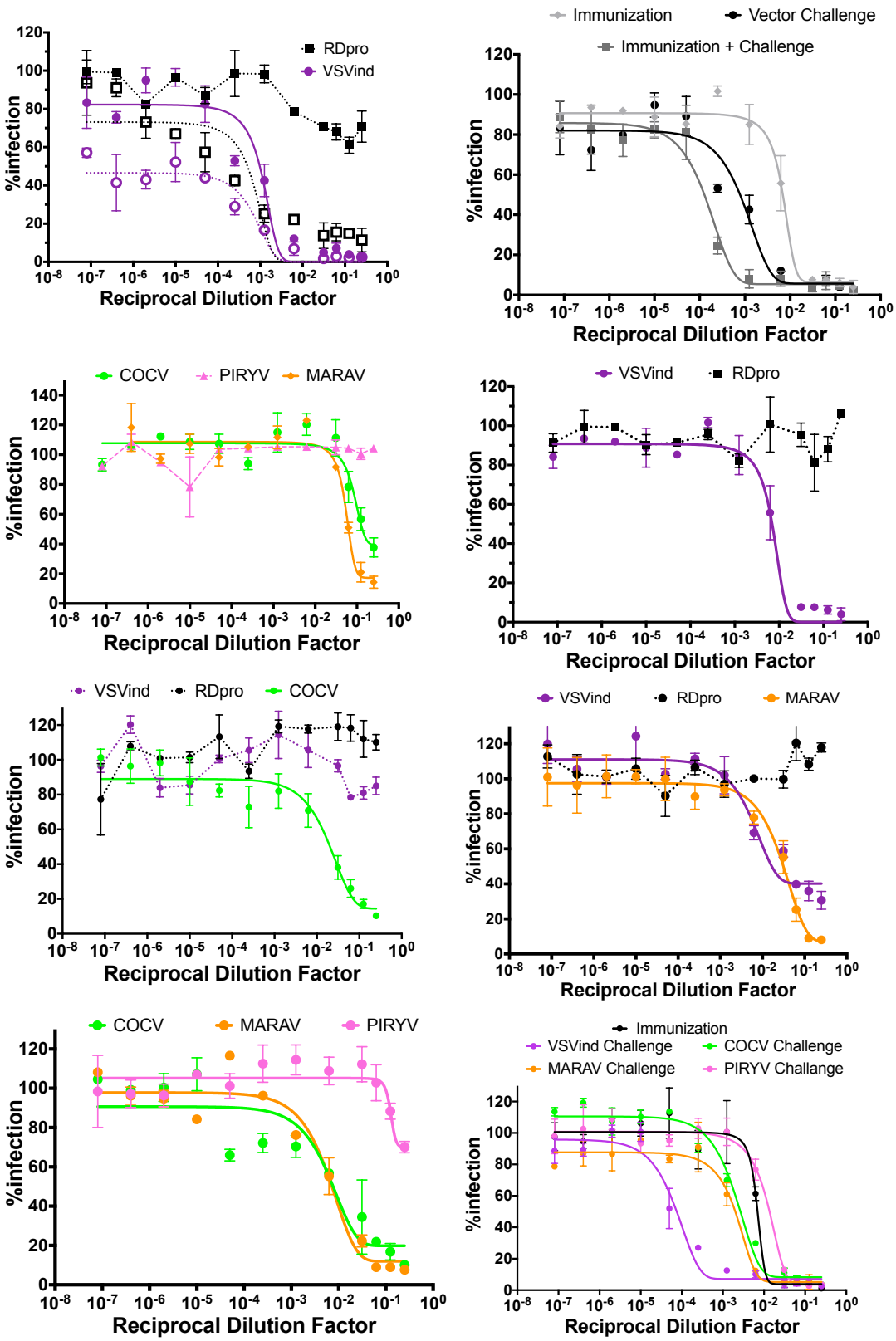

Supplementary Figure S3: Fitted Curves of the Neutralizations Assays Used to Calculate IC50 Values.

REFERENCES

1. Waterhouse, AM, Procter, JB, Martin, DMA, Clamp, M, and Barton, GJ (2009). Jalview Version 2-a multiple sequence alignment editor and analysis workbench. *Bioinformatics* **25**: 1189-1191.